

## Supporting Information

### **Raspberry-like morphology of polyvinyl chloride-zinc oxide nanoparticles induced by surface interaction for nanoporous foam**

Tingting Ren <sup>a</sup>, Jie Wang <sup>a</sup>, Jinfeng Yuan <sup>a</sup>, Mingwang Pan <sup>a,\*</sup>, Gang Liu <sup>a</sup>, Guanglin Zhang <sup>a</sup>, Gan-Ji Zhong <sup>b,\*</sup>, Zhong-Ming Li <sup>b</sup>

<sup>a</sup> Institute of Polymer Science and Engineering, Hebei University of Technology, Tianjin 300130, P. R. China.

E-mail: mwpan@126.com

<sup>b</sup> College of Polymer Science and Engineering, State Key Laboratory of Polymer Materials Engineering, Sichuan University, Chengdu 610065, Sichuan, P. R. China. E-mail: ganji.zhong@scu.edu.cn

#### **XPS characterization**

Figure S1 shows the XPS spectra of the surface of the P(VC-co-AAEM) particles with a couple of AAEM contents. The O1s spectrum of  $\beta$ -diketone hydrophilic groups and the Cl2p3 spectrum of PVC in the surface of the P(VC-co-AAEM) particles were clearly detected. When the AAEM/VC ratio was 6.0 g/ 60.0 g, the content of oxygen in the P(VC-co-AAEM) particles surface was 6.65% (Figure S1A), which was much higher than the calculated average content of oxygen (3.39%) in the P(VC-co-AAEM). In contrast, for the case of relatively larger AAEM/VC feed ratio of 12.0 g/ 60.0 g, the oxygen content in the P(VC-co-AAEM) particles surface was 12.14% (Figure S1B), which was also much higher than the calculated average content of oxygen (6.22%). Correspondingly, the chlorine content in the template surface obviously decreased from 39.03% to 24.42% with an increasing the AAEM content (Figure S1 A and B). Those experimental results confirmed that the  $\beta$ -diketone groups in AAEM were predominantly located onto the particle surface after the copolymerization process with vinyl chloride. Consequently, the hydrophilicity on the P(VC-co-AAEM) seeds surface can be enhanced by increasing the AAEM content.

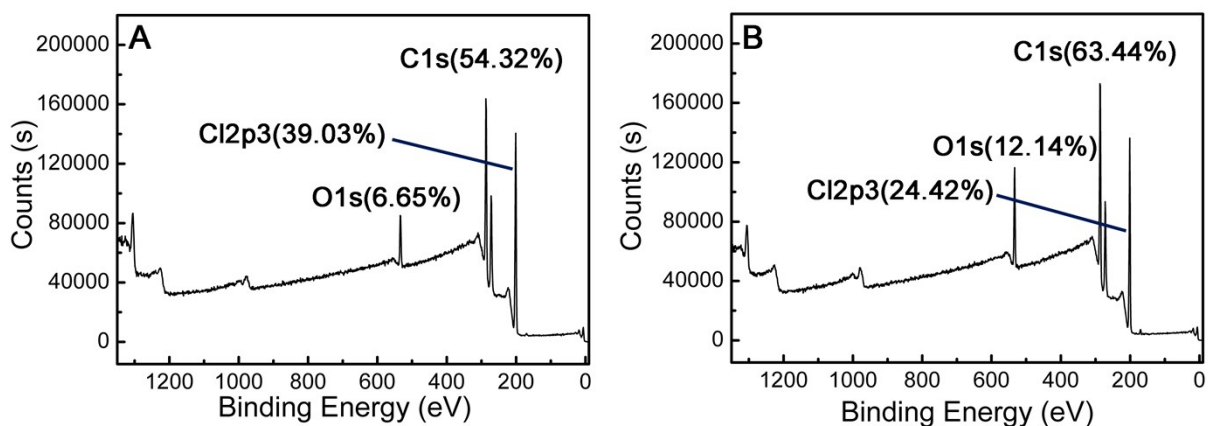


**Figure S1.** XPS spectra of the P(VC-co-AAEM) template particles. The AAEM/VC feed ratio for template preparation was (A) 6.0 g/ 60.0 g; (B) 12.0 g/ 60.0 g.

### Thermogravimetric Analysis (TGA) and Element Analysis

The data of TGA and element analysis for the P(VC-co-AAEM)/ZnO nanocomposites modified with ADC (i.e. sample A) are shown in Figure S2 and Table S1, respectively. In addition, the chemical structures of the used VC and AAEM monomers as well as both copolymer P(VC-co-AAEM) are also illustrated in Scheme S1.

It can be seen from Figure S2 that the final remainder content of sample A was 1.77 wt% in the air atmosphere, indicating the real ZnO content in sample A.

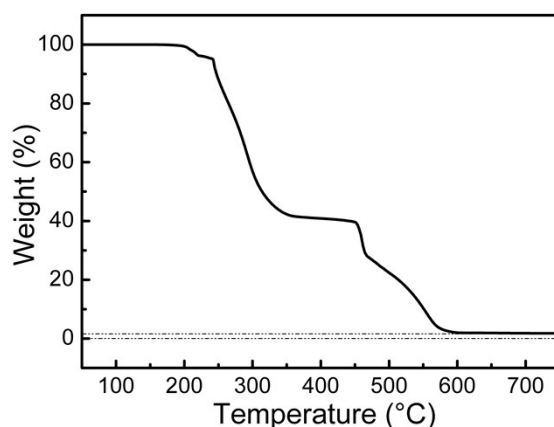


**Figure S2.** TGA curve for the P(VC-co-AAEM)/ZnO nanocomposites modified with ADC (Sample A)

**Table S1** Element analysis of Sample A



It can be seen from the inset in Figure S3 that the onset decomposition temperature of sample A was 192 °C, while that of sample B was 190 °C. At the first stage of thermogravimetric loss, the final decomposition temperature of sample A was 242 °C, and the corresponding residue amount was 95.2 wt%. While the final decomposition temperature of sample B was 241°C at the first stage of thermal weight loss, the corresponding residue amount was 94.7%. In comparison with their results by DSC analysis, as shown in Figure 12 of the revised manuscript, the decomposition temperature of sample A located between 176 °C and 203 °C, while one of sample B located between 184 °C and 210 °C. The difference between the DSC and TGA measurement results may be due to the different analysis methods and measure conditions. Generally, TGA records the change of sample weight loss along with an enhancement of temperature, whereas DSC measures the thermal enthalpy change from the physical and chemical change of the sample during heating process. In addition, as a kind of inorganic particles, the incorporation of ZnO particles could also improve the initial heat decomposition temperature of PVC.

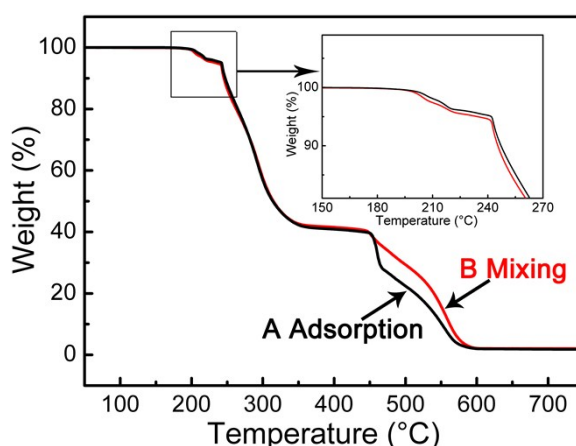


**Figure S3.** Thermal weight loss of A) the dissolving ADC into P(VC-co-AAEM)/ZnO composite (sample A) ; B) the blend of PVC, ZnO and ADC (sample B)

### Characterization of Foam Samples

The pore size distributions and some parameters of the foams from Samples A and B above were characterized by SEM study combined with mercury porosimetry test. And the cell size distributions of the foam materials (A and B) are shown in Figures S4 and S5. The detailed parameters of the corresponding foams are also summarized in Table S2.

The cell sizes and size distributions of the foams are determined by Image pro-plus 6.0 software to count the sizes of more than one hundred individual cells in the SEM micrographs. The cell density is calculated as the number of cells per unit volume with respect to the unfoamed polymer. The average cell size, standard deviation of cell size, and cell density are calculated by the following Equations (1) (2) and (3) (*Polym. Eng. Sci.*, 2002, 42, 1481-1492), respectively:

$$d = \frac{\sum d_i n_i}{\sum n_i} \quad (1)$$

$$S = \sqrt{\frac{1}{n-1} \sum_{i=1}^n (d_i - d)^2} \quad (2)$$

$$N_o = [nM^2/A]^{3/2} R_v \quad (3)$$

Where  $A$  is the area of the micrograph,  $\text{cm}^2$ ,  $d$  is the average cell size,  $\text{cm}$ .  $S$  is the standard deviation of cell size.  $N_o$  is the cell density,  $\text{cells}/\text{cm}^3$ .  $M$  is the magnification factor for the micrograph.  $n$  is the number of cells in the SEM micrograph, cells.  $R_v$  is the volume expansion ratio, %. The volume expansion ratio of each sample is calculated as the ratio of the bulk density of pure polyvinyl chloride material to the bulk density of the foam sample, namely:

$$R_v = \rho / \rho_f \quad (4)$$

$\rho$  is the density of the rigid (unfoamed) composite material,  $\text{g}/\text{mL}$ .  $\rho_f$  is the foam density,  $\text{g}/\text{mL}$ . The foam densities were tested by mercury porosimetry (AutoPore IV9500, Micromeritics, USA).

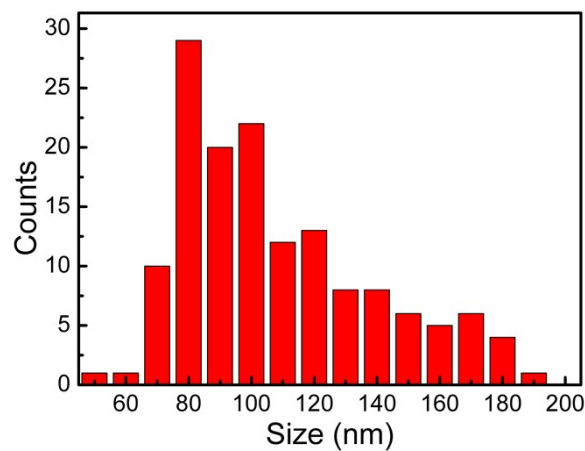


**Figure S4** Cell size distribution of the sample A foam

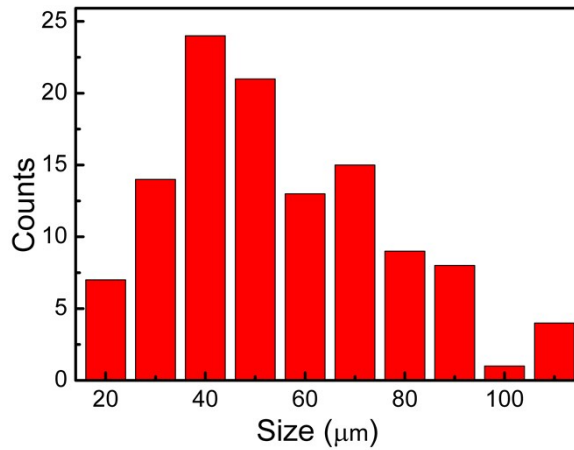


**Figure S5** Cell size distribution of the sample B foam

Comparing Figure S4 with Figure S5, it can be seen that the sample A foam presents nanometer sizes of pore distribution while the sample B foam exhibits micrometer sizes of pore distribution. Additionally, from Table S2, we can observe that the average pore size of the sample A foam is only 101 nm, but the average pore size of the sample B foam is 50.2 μm. In particular, the cell density in the sample A foam ( $3.8 \times 10^{13}$  cells/ cm<sup>3</sup>) is much larger than that in the sample B foam ( $5.4 \times 10^6$  cells/ cm<sup>3</sup>), resulting in probably lower foam density and better thermal insulation.

**Table S2** Parameters of the foams in detail

Sample	Average cell size	Standard deviation of cell size ( <i>S</i> )	Cell density (cells/cm <sup>3</sup> )	Foam density (g/mL)	Expansion ratio
A	101 nm	42.8	$3.8 \times 10^{13}$	1.221	1.19
B	50.2 μm	22.2	$5.4 \times 10^6$	1.248	1.20